

Article

Not peer-reviewed version

---

# Isolation and Characterization of a Novel Pseudorabies Virus Variant Strain in Gansu Province, China, 2021

---

[Xiaobing He](#), Hua Yang, [Peng Ji](#), Guohua Chen, Yongxiang Fang, Zhizhong Jing, [Yanming Wei](#)\*

Posted Date: 17 March 2025

doi: 10.20944/preprints202503.1223.v1

Keywords: pseudorabies virus; variant strain; biological characteristics; genetic evolution; pathogenicity; Gansu province



Preprints.org is a free multidisciplinary platform providing preprint service that is dedicated to making early versions of research outputs permanently available and citable. Preprints posted at Preprints.org appear in Web of Science, Crossref, Google Scholar, Scilit, Europe PMC.

Copyright: This open access article is published under a Creative Commons CC BY 4.0 license, which permit the free download, distribution, and reuse, provided that the author and preprint are cited in any reuse.

Article

# Isolation and Characterization of a Novel Pseudorabies Virus Variant Strain in Gansu Province, China, 2021

Xiaobing He <sup>1,2,3,4</sup>, Hua Yang <sup>5</sup>, Peng Ji <sup>1</sup>, Guohua Chen <sup>2,3,4</sup>, Yongxiang Fang <sup>2,3,4</sup>, Zhizhong Jing <sup>2,3,4</sup> and Yanming Wei <sup>1,\*</sup>

<sup>1</sup> College of Veterinary Medicine, Gansu Agricultural University, Lanzhou 730070, China; hexiaobing@caas.cn;

jipengjipeng528@163.com

<sup>2</sup> State Key Laboratory for Animal Disease Control and Prevention, Lanzhou Veterinary Research Institute, Chinese

Academy of Agricultural Sciences, Lanzhou 730046, China; chenguohua02@caas.cn; fangyongxiang@caas.cn;

zhizhongjing@caas.cn

<sup>3</sup> Gansu Province Research Center for Basic Disciplines of Pathogen Biology, Lanzhou 730046, China

<sup>4</sup> Key Laboratory of Veterinary Etiological Biology and Key Laboratory of Ruminant Disease Prevention and Control

(West), Ministry of Agricultural and Rural Affairs, Lanzhou 730046, China

<sup>5</sup> Gansu Vocational College of Agriculture, Lanzhou 730030, China; yanghua@163.com

\* Correspondence: Weiyim@gsau.edu.cn

**Abstract:** The outbreaks of pseudorabies (PR) caused by the pseudorabies virus (PRV) variant strains have led to huge economic losses to the pig industry in China in recent years. In this study, a novel PRV variant strain named PRV/Gansu/China/2021 (GS-2021) was successfully isolated and identified from the brain tissue samples of PRV-suspected dead piglets at a Bartha-K61-vaccinated pig farm in Gansu Provinces, China, in 2021, and its biological characteristics, genetic features, evolutionary relationship and pathogenicity were further evaluated. The results showed that the PRV GS-2021 strain had different plaque sizes but no significant difference in replication kinetics with Bartha-K61 strain *in vitro*. In addition, sequence alignments revealed that the gB, gC, gD, and gE proteins of PRV GS-2021 strain shared highly homologous to those of the variant strains. However, glutamate was replaced by glycine at position 91 in the gE protein of the viral strain, although two aspartate insertions were detected at sites 48 and 498 in the gE protein of the virus. Phylogenetic analysis found that it was more closely related to endemic PRV strains, particularly the variant strains circulating in China, based on those *gB*, *gC*, *gD*, and *gE* genes and complete genome sequence. Moreover, we further discovered that the PRV GS-2021 strain exhibited a higher pathogenicity than the Bartha-K61 strain in mice through mortality, histopathology, and viral loads. Overall, our results suggested that the isolated PRV GS-2021 strain as a higher virulence variant, has prevalent in Gansu province of China before 2021 and these findings are important for continuously monitoring the epidemiological characterization and genetic evolution of PRV, which will provide a useful guidance for the design of novel vaccines and more efficacious control and prevention strategies of PR in the future.

**Keywords:** pseudorabies virus; variant strain; biological characteristics; genetic evolution; pathogenicity; Gansu province

## 1. Introduction

Pseudorabies virus (PRV), also known as Aujeszky's disease virus (ADV) or suid herpesvirus type 1 (SuHV-1), belongs to the genus *Varicellovirus* of the subfamily *Alphaherpesvirinae* with the family *Herpesviridae*. PRV is an enveloped virus with a large double-stranded linear DNA genome of approximately 150 kb in length and encodes at least 70 proteins [1,2]. PRV is the causative agent of Pseudorabies (PR) or Aujeszky's disease (AD), and it has the capacity to infect a wide variety of

wildlife, domestic animals, and livestock, including ruminants, carnivores, and rodents. However, pigs constitute the sole natural reservoir for PRV, and the host to become latent carriers, which can lead to acute infection and great economic losses in the swine industry worldwide, particularly in developing countries [1,2]. PRV is a highly neurotropic virus that causes neurological disorders and frequently results in a high rate of mortality in newborn piglets. Conversely, older pigs usually exhibit subclinical symptoms such as respiratory disturbance, malaise and decreased appetite. Furthermore, PRV infections in pregnant sows may lead to breeding obstacles, including stillbirths, abortions, and weakling piglets [1,2]. Following the acute stage of infection, PRV can establish a latent infection that persists throughout the life of the infected pig. However, it is noteworthy that latently infected pigs can be re-infected due to the spontaneous reactivation of the latent viral genome or reactivation by stress, a phenomenon that weakens the immune system of latently infected pigs, thereby facilitating a more severe infection [1,2].

In China, PR was effectively mitigated through the implementation of extensive vaccination programmes in swine populations using the Bartha-K61 vaccine from the early 1990s until late 2011. However, by the conclusion of 2011, a significant resurgence of PR outbreaks had occurred on numerous Bartha-K61 vaccinated swine farms, rapidly disseminating to various regions across China and resulting in substantial economic losses [3,4]. It had been demonstrated that the traditional Bartha-K61 vaccine was incapable of providing complete protection against novel emerging PRV strains in China [5]. Genetic analysis revealed several mutations in most viral proteins of the PRV variants, including substitutions, insertions and/or deletions. These findings indicated that novel emerging PRV variant strains had begun to circulate among populations of infected pigs in China [6,7]. Furthermore, studies have indicated that increased virulence and antigenic variation of the novel PRV mutant strains are the primary cause of the serious spread in China, which could explain why there have been large-scale outbreaks of PRV variant strains in China since late 2011[6-8]. Consequently, much attention has been focused on how to prevent and control the recurrence of this disease. Notably, more than 30 clinical cases of PRV infection in humans so far have been reported in China [11-14]. Moreover, A human-originated PRV variant strain, designated hSD-1/2019, was successfully isolated from a patient with cerebrospinal fluid in 2019, providing direct evidence of PRV infection in humans, thus classifying the PRV variant strain as an emerging zoonotic pathogen [15,16]. However, epidemiological data, genomic characterization, and pathogenicity of the PRV variant strains currently circulating in China, especially in Gansu Province, remain limited. In the present study, a novel PRV variant strain, designated as PRV/Gansu/China/2021, was isolated and identified from a PRV-suspected clinical brain tissue sample from deceased piglets on a Bartha-K61-vaccinated pig farm in Gansu Province, China, in 2021 and further investigation was conducted to ascertain the biological characteristics, genetic features and evolution, and pathogenicity of the strain in mice. Our results suggest that the PRV GS-2021 is a higher virulence variant strain and could have already circulated in Gansu Province of China before 2021.

## 2. Materials and Methods

### 2.1. Cells, Viruses, Antibodies, and Animals

The propagation or titration of the virus was carried out in Vero cells (SCSP-520, CAS, China) and PK-15 cells (CCL-33, ATCC, USA) with Dulbecco's modified Eagle medium (DMEM) (11995073, Gibco, China) containing 10% fetal bovine serum (10091148, Gibco, New Zealand) at 37 °C in 5 % CO<sub>2</sub>. The PRV vaccine strain Bartha-K61 was isolated from a commercial vaccine and used as a control virus, while brain tissue from specific-pathogen-free (SPF) piglets used as a negative control. The primary antibodies employed in this study were rabbit anti-pseudorabies virus gB antiserum (PSRVGB11-S, Alpha Diagnostic International, USA) and rabbit anti-pseudorabies virus antibody (ab3534, Abcam, USA). The secondary antibodies employed were goat anti-rabbit IgG alexa fluor®488 (H+L) (GB25303, Servicebio, China) and goat anti-rabbit IgG alexa fluor®594 (H+L) (GB28301, Servicebio, China). Adult BALB/c mice (6–8 weeks, 16–20 g body weight) from the Animal Experimental Center of the Lanzhou Veterinary Research Institute, Chinese Academy of Agricultural Sciences.

## 2.2. Clinical Sample Collection and Virus Detection

Clinical brain samples were obtained from PRV-suspected dead piglets on a Bartha-K61-vaccinated pig farm in Gansu Province, China, in 2021. The brain samples were then homogenized in DMEM at 4 °C, after which the DNA was extracted from the tissue homogenate using a Viral RNA/DNA Extraction Kit (9766, TaKaRa, Japan). The primers for the partial gB and gE gene fragments of PRV were designed according to the PRV gene sequence on GenBank (GenBank accession number: KP722022). The amplified fragments of the target genes were 282 bp and 258 bp. The extracted DNA samples were identified with polymerase chain reaction (PCR) using PRV gB and gE-specific pairs primers (Table 1). The PCR products were then subjected to agarose gel electrophoresis to confirm their identity.

**Table 1.** Primers used in this study.

Reference Sequence	Gene	Primer Sequence (5' - 3')	Length
KP257591	gB	TGTACCTGACCTACGAGGCGTCATG GTGGGAGCCGTCACACGCGCCAGC	2818 bp
KP257591	gC	TGTGTGCCACTAGCATTAAATCCGTT GTTCAACGCGCGGTTCGTTTATTGAT	1605 bp
KP257591	gD	ATACACTCACCTGCCAGCGCCATG ACCATCATCATCGACGCCGGTACT	1262 bp
KP257591	gE	GTTGAGACCATGCGGCCCTTCT GGACCGTTCTCCCGGTATTTAAG	1786 bp
KP257591	gE	TGCCACGCACGAGGACTACTACG CGCCATAGTTGGGTCCATTCGTCAC	258 bp
KP257591	gB	TGCAGAACAAGGACCGCACCCCTGT GCGAGATGAGGAGCTCGTTGTCGT	282 bp
KP257591	gB	AAGTTCAAGGCCACATCT TGAAGCGGTTCTGTGATGG	88 bp
		FAM-CAAGAACGTCATCGTCACGACCG- BHQ	

## 2.3. Viral Isolation and Identification

PRV PCR gB and gE-positive homogenates were treated with antibiotics and subjected to a centrifugation process at 5000 g/min for 15 min at 4 °C. Subsequently, the resultant filtrate was filtered through a 0.45-µm filter (0000240486, Merck Millipore, Germany) and inoculated into a monolayer of Vero cells. The cells were then incubated in Minimum Essential Medium (MEM) (11095080, Gibco, USA) with 1% FBS in a 5% CO<sub>2</sub> incubator at 37 °C. The presence of a cytopathic effect (CPE) was examined daily, and the observation of cell morphology and the anchorage-dependent rate were recorded using a microscope. At 85-95% CPE, the Vero cells were subjected to freeze-thaw cycles with the culture medium, after which the cell culture medium was collected. Following amplification, cultivation and six rounds of plaque purification, the virus was identified using PCR and Sanger sequencing, indirect immunofluorescent assay (IFA) and transmission electron microscope (TEM) system HT7800 (Hitachi, Japan).

## 2.4. Plaque Assay and Plaque Sizes Determination

Vero cells were seeded in 12-well plates, after which a serial 10-fold dilution of the virus was added to the cells. Following a one-hour incubation period, the cells were washed three times with PBS and overlaid with 0.75% carboxy methyl cellulose (M352, Fisher Scientific, USA) in DMEM

medium containing 2% FBS. The plates were then incubated at 37°C for 2–3 days until visible plaques formed. The cells were then fixed using 4% paraformaldehyde (252549, Sigma-Aldrich, USA) and then stained with 500 µl of crystal violet (C0775, Sigma-Aldrich, USA). The plaque-forming units (PFU) of the isolated PRV GS-2021 strain were then calculated by plaque assay. Fifty plaques of each virus were randomly selected, and their diameters were measured using ImageJ software. The relative diameter of the plaque was then calculated as the product of the diameter of the PRV GS-2021 strain divided by those of the Bartha-K61 strain.

### 2.5. One-Step Growth Curve of the PRV GS-2021 Strain

Vero cell monolayers in 12-well plates were infected with the virus at an MOI of 1. Following incubation at 37°C for 1 h, the medium was replaced with DMEM containing 2% FBS. The cells and the remaining fluid were harvested at 6-, 12-, 24-, 36-, and 48-hour post-infection (hpi) and stored in aliquots at –80°C. Following three freeze-thaw cycles, the virus was tittered by the plaque formation assay in Vero cells.

### 2.6. Amplification and Sequencing of gB, gC, gD, and gE Genes of the PRV GS-2021 Strain

The complete gB, gC, gD, and gE genes of PRV strain were amplified by PCR through specific primers (Table 1). The PCR reaction was conducted in the volume of 100 µl containing 20 ng of extracted DNA, 20 µl 5 × PrimerSTAR GXL Buffer, 2 µl PrimeSTAR GXL DNA polymerase (R050A, TaKaRa, China), 8 µl 2.5 mM deoxynucleoside triphosphate (dNTP), 0.25 µM of each primer, add Nuclease-free water supplement to 100 µl. Thermal cycling parameters were 95 °C for 4 sec, then 35 cycles of denaturation at 98 °C for 10 sec, annealing at 55 °C for 10 sec, and extension at 68 °C for 3 min 20 sec, followed by final extension at 72 °C for 10 min. The purified PCR products were connected to the pJET1.2 vector with the Clone JET PCR Cloning Kit (K1231, Thermo Scientific, USA) and verified by sequencing to obtain the final assembly results.

### 2.7. Complete Genome Sequencing of the PRV GS-2021 Strain

The whole-genome of the purified PRV GS-2021 strain was sequenced through next-generation sequencing (NGS) technology on PE150 platform with a high-throughput the Illumina Nova 6000 (Magigen Biotech, Guangzhou, China). To assemble the genome, reads were mapped to the reference genome (GenBank accession number: KP722022) and the assembled whole genomic sequence.

### 2.8. Phylogenetic Analyses of the PRV GS-2021 Strain

Forty-one genome sequences of PRV representing wild strains or vaccine strains from different endemic countries were obtained from GenBank (Table 1). The sequence was compared to those of viral strains from different endemic countries. The sequences alignment of the nucleic acid and amino acid sequences were conducted by MegAlign module in DNASTAR Lasergene 7 software. Phylogenetic trees were also calculated using the maximum-likelihood method of the MEGA-X software based on the General-Time-Reversible model for the gB gene sequences, the General-Time-Reversible with Invariant Sites Substitution model for the gC gene sequences, the Hasegawa-Kishino-Yano with Invariant Sites substitution model for the gD gene sequences, the General-Time-Reversible model for the gE gene sequences, and the General-Time-Reversible with Gamma Distribution Substitution model for the complete genomic sequences, and bootstrap values were calculated with 1000 replicates.

**Table 2.** PRV reference strains in this study.

Strain	Accession Number	Genotype (I/IIa/IIb)	Country	Species	Isolate Date
TJ	KJ789182	IIb	China	Swine	2012
ZJ01	KM061380	IIb	China	Swine	2012
HNX	KM189912	IIb	China	Swine	2012

HNB	KM189914	IIb	China	Swine	2012
HeN1	KP098534	IIb	China	Swine	2012
JS-2012	KP257591	IIb	China	Swine	2012
DX	OK338076	IIb	China	Swine	2012
HLJ8	KT824771	IIb	China	Swine	2013
GD-YH	MT197597	IIb	China	Swine	2014
HN1201	KP722022	IIb	China	Swine	2015
XJ	MW893682	IIb	China	Dog	2015
JS-XJ5	OP512542	IIb	China	Swine	2016
JX	MK806387	IIb	China	Swine	2016
HeNZM	MT775883	IIb	China	Swine	2017
HeNLH	MT775883	IIb	China	Swine	2017
JSY13	MT157263	IIb	China	Swine	2018
HuBXY	MT468549	IIb	China	Swine	2018
FJ	OP727803	IIb	China	Tiger	2018
FJ	MW286330	IIb	China	wine	2019
SX1910	OL606749	IIb	China	Swine	2019
hSD-1	MT468550	IIb	China	Human	2019
SD18	MT949536	IIb	China	Swine	2020
GD	OK338076	IIb	China	Swine	2020
JM	OK338077	IIb	China	Swine	2021
CD22	OR666765	IIb	China	Swine	2022
HLJPRVJ	OR365764	IIb	China	Swine	2023
DCD-1	OL639029	IIb	China	Swine	2017
HLJ-2013	MK080279	IIa	China	Swine	2013
GXGG	OP605538	IIa	China	Swine	2016
HuB17	MT949537	IIa	China	Swine	2020
JS-2020	OR271601	IIa	China	Swine	2020
SC	KT809429	IIa	China	Swine	1986
Ea	KU315430	IIa	China	Swine	1990
LA	KU552118	IIa	China	Swine	1997
Fa	KM189913	IIa	China	Swine	2012
MY-1	AP018925	IIa	Japan	Swine	2015
Kolchis	KT983811	I	Greece	Tiger	2010
Bartha	JF797217	I	Hungary	Swine	1960
Kaplan	JF797218	I	Hungary	Swine	2011
Becker	JF797219	I	USA	Swine	1967
NIA3	KU900059	I	UK	Swine	2016

### 2.9. Challenge of Mice with the PRV GS-2021 Strain

For the pathogenicity of the PRV GS-2021 strain, 24 six-week-old specific-pathogen-free (SPF) BALB/c mice were intranasally (I.N.) injected with  $10^4$ ,  $10^3$ , and  $10^2$  PFU of the variant strain in 10  $\mu$ l DMEM. At the same time, 32 mice were designated as controls and injected with  $10^6$ ,  $10^5$ , and  $10^4$  PFU of the Bartha-K61 strain and equivalent volume of DMEM. After inoculation, the mice were observed

each day for clinical symptoms and death, and lethal dose (LD<sub>50</sub>) of the virus strains were calculated by the Spearman-Kärber method. Liver, spleen, lung, brain and/or blood were collected from the GS-2021 and Bartha-K61-infected mice at 3rd day post-infection for hematoxylin and eosin (H&E) staining and IFA, and the virus was detected using gB-specific TaqMan quantitative PCR (Table 1).

### 2.10. Statistical Analysis

Data were presented as mean  $\pm$  standard error of the mean from 3 independent assays. Statistical analyses were performed using GraphPad Prism version 5.0 software. The significance of differences between groups was evaluated using a student's t-test or 2-way analysis of variance. A p-value of less than 0.05 was considered statistically significant: \*,  $p < 0.05$ ; \*\*,  $p < 0.01$ ; \*\*\*,  $p < 0.001$ ; \*\*\*\*,  $p < 0.0001$ .

## 3. Results

### 3.1. Detection of PRV in Clinical Brain Tissue by PCR

The sick piglets in one farm in Wuwei (Gansu Province, China) presented with multiple clinical signs, including high fever ( $\geq 40.5$  °C), depression, inappetence, weight loss, dyspnea, chilling, vomiting, secretion discharged from mouth and systemic neurological symptoms. Viral genome DNA was extracted from clinical brain tissue samples, and the partial gB gene and gE gene of PRV was amplified by PCR method. As shown in Figure 1, PRV-suspected brain samples were verified to be gB gene and gE gene positive, but the gE gene were negative for PRV Bartha-K61 genome as a positive control and brain sample from a healthy piglet as a negative control, suggesting the dead piglets on the Bartha-K61-vaccinated farm were infected with the PRV field strain.

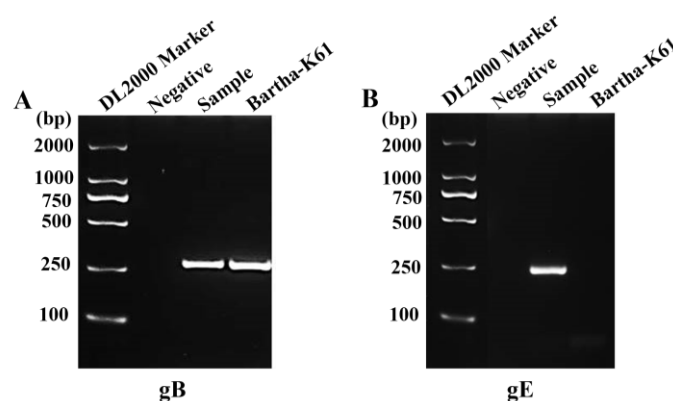


**Figure 1.** Detection of the PRV gB or gE genes in clinical brain samples by PCR. (A) Amplified PCR product of partial PRV gB gene (258 bp). (B) Amplified PCR product of partial PRV gE gene (282 bp). Negative sample from a specific-pathogen-free (SPF) piglet used as negative control and Bartha-K61 used as positive control.

### 3.2. Isolation and Identification of the PRV GS-2021 Strain

The PRV gB gene and gE gene-positive tissue samples were processed and inoculated into Vero cells, and obvious cytopathic effect (CPE) were characterized by shrink, reduced in size and turned rounded with loose arrangement and poor adhesiveness, which were like those of Bartha-K61 strain with the PRV-positive homogenate 18 hr postinfection (Figure 2A). In addition, gB-specific fluorescence signals appeared in the cytoplasm and nucleus of PRV-infected Vero cells by IFA (Figure 2A). Meanwhile, the herpesvirus-like virus particles can be detected in the Vero cells infected with PRV isolate and Bartha-K61 by TEM (Figure 2A), and the virus particles of sucrose density-gradient centrifugation with a diameter of 81~133 nm also were also exhibited spherical envelope protein with a radially arranged spike by TEM (Figure 2A), which is consistent with the morphology of PRV. However, there was no obvious difference in the morphology between the isolated PRV and Bartha-K61 strain. Moreover, viral genome DNA was extracted from PRV and the complete gC and gE genes were still positive with PCR and further confirmed by Sanger sequencing (Figure 2C). These results indicated that a field PRV strain was successfully isolated from the clinical samples on a Bartha-K61-vaccinated swine farm and named PRV/Gansu/China/2021 (also called PRV GS-2021).

### 3.3. Biological Characteristics of the PRV GS-2021 Strain

Plaque assay and one-step growth curve experiments were performed to investigate the growth characteristics of the PRV GS-2021 strain, and the Bartha-K61 vaccine strain were set as control groups. The viral titers of the GS-2021 and Bartha-K61 were  $1.15 \times 10^7$  PFU/ml and  $1.5 \times 10^6$  PFU/ml, respectively. The GS-2021 strain developed a plaque area significantly larger than that of the Bartha-K61 strain (Figure 3A, B), suggesting a much stronger virus spreading of the GS-2021 strain than that of the Bartha-K61 strain in Vero cells. Furthermore, one-step growth curve analysis revealed that the GS-2021 strain displayed similar growth kinetics and a replication superiority at the end time point compared with the Bartha-K61 strain in Vero cells (Figure 3C). However, the Bartha-K61 strain propagated slightly faster than the GS-2021 strain in PK-15 cells (Figure 3D), which may be attributed by the better adaptation of Bartha-K61 in this cell line. These results showed that the PRV GS-2021 strain had different plaque sizes but no significant difference in replication kinetics with the Bartha-K61 strains.

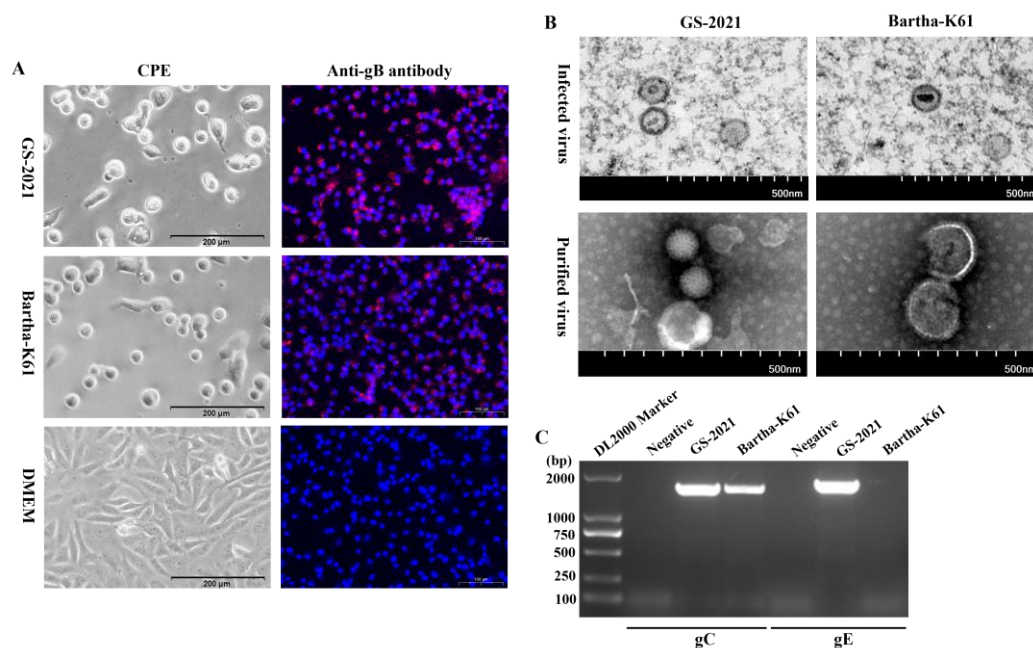


**Figure 2.** Isolation and identification of PRV GS-2021 strain. (A) The cytopathic effect (CPE) of Vero cells caused by GS-2021. The CPE in Bartha-K61-infected Vero cells was considered as positive control (left panels). Indirect immunofluorescence assay detection of gB (green) protein in GS-2021 or Bartha-K61-challenged Vero cells, and the nucleus was stained with DAPI (right panels). (B) Viral particles in Vero cells (top panel) or purified virus (bottom panel) of GS-2021 and Bartha-K61 under the transmission electron microscope. (C) PCR amplification of PRV gC (1605 bp) and gE (1786 bp) fragments from passage 6 cultures of GS-2021-inoculated Vero cells. Bartha-K61 was positive control and DMEM was negative control.

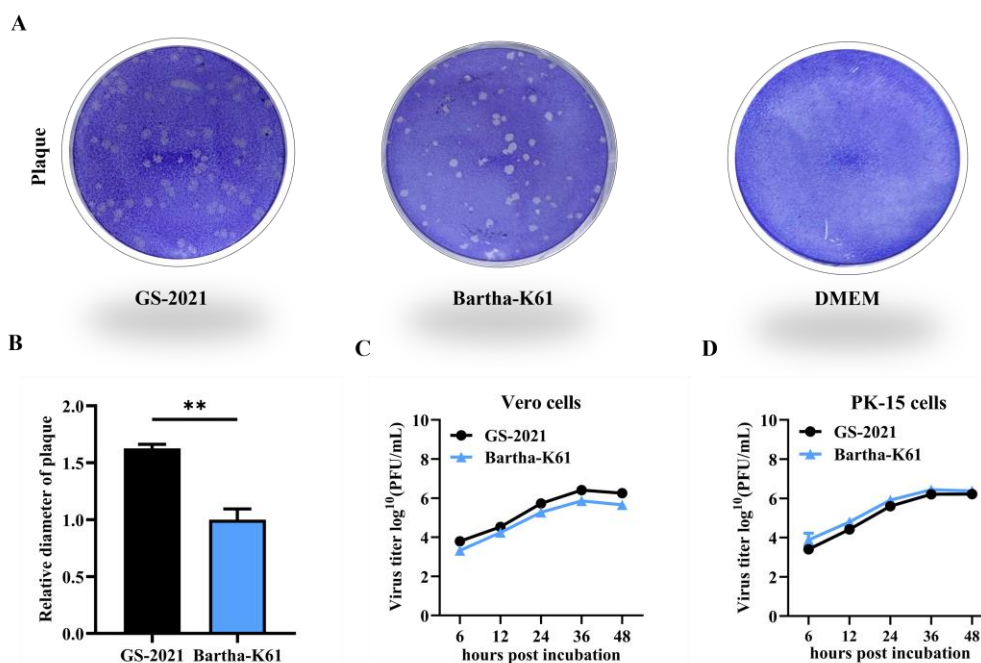


**Figure 3.** Biological characteristics of the PRV GS-2021 strain in vitro. (A) Plaque formation in Vero cells infected by the GS-2021 and Bartha-K61. (B) The relative plaque size of each virus was normalized to that of Bartha-K61. Significant differences were considered: \*\*P < 0.01. (C, D) One-step growth curves of the two PRV strains in Vero cells and PK-15 cells at an MOI of 1, respectively, and the viral titers were determined in Vero cells by plaque assay method.

### 3.4. Genetic Features of the PRV GS-2021 Strain

To identify the genetic characteristics of the PRV GS-2021 strain, the complete genome sequences were sequenced by using the high-throughput sequencing method. The complete genome of the GS-2021 strain was comprised of 142,532 bp, which encodes 88 open reading frames (ORFs). The GC content in whole genome of the GS-2021 strain is 73.61%, which was like other published PRV strains (Table 3). Compared with the complete genome sequences of other PRV, we found the homology of the PRV GS-2021 strain with Chinese PRV variant strains such as HN1201, SX1910, HLJ8, DCD-1 and hSD-1 are 99.96%, 99.96%, 99.94%, 99.93% and 99.91%, respectively, the homology of the PRV GS-2021 strain with Chinese classical PRV isolates Fa, Ea, LA and SC are 99.48%, 99.27%, 98.98% and 98.60%, respectively, the homology of the PRV GS-2021 strain with classical foreign PRV strains Kolchis, Kaplan, Bartha, Becker and NIA3 are 97.31%, 97.11%, 96.20%, 96.11% and 96.02%, respectively (Table 4). However, the PRV GS-2021 strain had higher homology with the HN1201 and SX1910 strains isolated in 2015 and 2019, respectively (Table 4), suggesting the PRV GS-2021 strain may be originate from the HN1201 strain in Henan of China or SX1910 strain in Shanxi of China through illegal transportation across provinces.

**Table 3.** PRV reference strains in this study.

Strain	Complete Genome	T(%)	C(%)	A(%)	G(%)	G+C(%)	A+T(%)
TJ	143642	13.27	36.94	13.10	36.69	73.63	26.37
ZJ01	141028	13.20	36.97	13.06	36.76	73.74	26.26
HNX	142294	13.30	36.82	13.14	36.74	73.56	26.44
HNB	142255	13.27	36.87	13.12	36.74	73.61	26.39
HeN1	141803	13.26	36.96	13.05	36.73	73.69	26.31
JS-2012	145312	13.29	36.78	13.21	36.73	73.50	26.50

DX	143754	13.27	36.83	13.14	36.76	73.59	26.41
HLJ8	142298	13.22	36.91	13.08	36.79	73.70	26.30
GD-YH	146012	13.17	36.83	13.07	36.93	73.76	26.24
HN1201	144173	13.27	36.81	13.18	36.73	73.54	26.46
XJ	144483	13.28	36.89	13.13	36.71	73.60	26.40
JS-XJ5	141955	13.22	37.05	12.99	36.75	73.79	26.21
JX	143156	13.32	36.89	13.12	36.68	73.57	26.43
HeNZM	144235	13.33	36.61	13.09	36.98	73.58	26.42
HeNLH	143254	13.21	37.04	13.01	36.74	73.78	26.22
JSY13	143452	13.17	36.98	13.01	36.84	73.82	26.18
HuBXY	143859	13.22	36.83	13.04	36.92	73.75	26.25
FJ	144795	13.23	36.79	13.14	36.84	73.63	26.37
FJ	142763	13.19	36.86	13.43	36.52	73.38	26.62
SX1910	143703	13.23	36.78	13.14	36.84	73.62	26.38
hSD-1	143236	13.25	36.88	13.12	36.75	73.63	26.37
SD18	143905	13.24	36.87	13.10	36.79	73.66	26.34
GD	143418	13.27	36.93	13.10	36.70	73.63	26.37
JM	144046	13.19	36.92	13.06	36.83	73.75	26.25
CD22	142472	13.23	37.05	13.03	36.69	73.74	26.26
HLJPRVJ	143520	13.29	36.93	13.10	36.69	73.61	26.39
DCD-1	143218	13.20	36.93	13.07	36.81	73.73	26.27
HLJ-2013	142560	13.23	36.95	13.09	36.73	73.67	26.33
GXGG	142288	13.25	36.89	13.08	36.77	73.67	26.33
HuB17	141631	13.19	37.06	13.03	36.72	73.78	26.22
JS-2020	143246	13.27	36.88	13.10	36.74	73.62	26.38
SC	142825	13.26	36.93	13.13	36.68	73.61	26.39
Ea	142334	13.28	36.89	13.12	36.72	73.60	26.40
LA	141428	13.28	36.97	13.06	36.69	73.66	26.34
Fa	141930	13.25	36.89	13.06	36.80	73.70	26.30
MY-1	143277	13.28	36.83	13.14	36.75	73.58	26.42
Kolchis	141542	13.23	37.11	13.08	36.58	73.69	26.31
Bartha	137764	13.19	36.98	13.10	36.73	73.71	26.29
Kaplan	140377	13.22	37.05	13.10	36.63	73.68	26.32
Becker	141113	13.15	37.00	13.11	36.74	73.74	26.26
NIA3	142228	13.15	36.97	13.11	36.77	73.74	26.26

Besides, the gB, gC, gD, and gE genes of the GS-2021 strain were amplified by PCR and then analysis with the sequences of PRV in the GenBank database (Table 2). The gB, gC, and gD genes of the GS-2021 strain shared 100% nucleotide sequence homologous with most of the PRV variant strains isolated from different regions in China (Table 4). However, gB, gC, and gD genes shared more than 99.3% nucleotide sequence homology with Chinese classical PRV strains, but those were lower than 99.3% nucleotide sequence homology with foreign strains. Additionally, the gE gene has not shown 100% nucleotide sequence homologous with Chinese variant strains (Table 4). Compared with earlier PRV strains from China and other country, the gE protein of the PRV Chinese variant strains have two Aspartate (Asp, D) insertions at site 48 and 497, respectively (Figure 4). Notably, two Asp insertions are also detected in the gE protein of the PRV GS-2021 strain and glutamate is

replaced by glycine at position 91 (Figure 4). Nevertheless, two Asp insertions have been observed in an earlier LA strain from China, this shows that the two insertions have occurred previously. These results showed that the PRV GS-2021 might be a variant PRV strain.

**Table 3.** Comparison of complete genome and gB, gC, gD, and gE genes sequences of the PRV strains.

Comparison with the PRV GS-2021 Strain			Nucleotide Sequence (%)				
			Genome Sequence	gB	gC	gD	gE
Chinese strains	variant PRV	99.59-99.96	99.90- 100.00	99.90- 100.00	99.80- 100.00	99.70- 99.90	
Chinese strains	classical PRV	98.40-99.48	99.30- 99.80	96.90- 99.70	99.50- 99.70	99.70	
Foreign strains	classical PRV	96.02-97.31	98.40- 98.50	94.90- 96.30	98.90- 99.30	97.70- 98.0	



**Figure 4.** Comparative sequence alignment of PRV gE proteins. 42 gE amino acid sequences of the PRV strains with complete genome sequences are available in GenBank and were compared using DNASTAR Lasergene 7 software and the sequences were aligned using the Clustal W method.

### 3.5. Phylogenetic Analysis of the PRV GS-2021 Strain

To investigate the phylogenetic relationship between the PRV GS-2021 strain and other PRV strains published in GenBank (Table 2), a phylogenetic tree was constructed based on the 42 complete genome sequences. Phylogenetic analysis showed that the PRV strains was divided into two main evolutionary clades: Clade I was composed of classical PRV strains from other countries, and Clade II was composed of the PRV isolates from China such as the Chinese classical PRV strains and the PRV variant strains (Figure 5A). However, within clade II, the PRV GS-2021 strain was more closely

related to the Chinese PRV variant strains, including HN1201, SX1910, HLJ8, DCD-1 and hSD-1, than the Chinese classical PRV strains, such as Fa, Ea, LA and SC. Therefore, clade II is subdivided into two subclades, IIa and IIb. Clade IIa is composed of the Chinese classical PRV strains, and Clade IIb is composed of the Chinese PRV variant strains, which was responsible for the ongoing outbreak from 2011 to 2024 in China [6, 7, 13]. In addition, the phylogenetic tree of the 42 complete nucleotide sequences based on gB, gC, gD, and gE gene sequences showed that PRV was also divided into two distinct clades: Chinese PRV strains including Chinese classical PRV strains (IIa) and PRV variant strains (IIb) clustered into the clade II, which was mainly composed of strains from China, and the other clade was mainly composed of European and American strains (Figure 5B-E). Among clade II, the PRV GS-2021 strain was clustered together with Chinese variants and especially more closely related to the variant named HN1201, SX1910, HLJ8, DCD-1 and hSD-1 strains that had emerged in recent years, also formed IIb clade (Figure 5B-E).

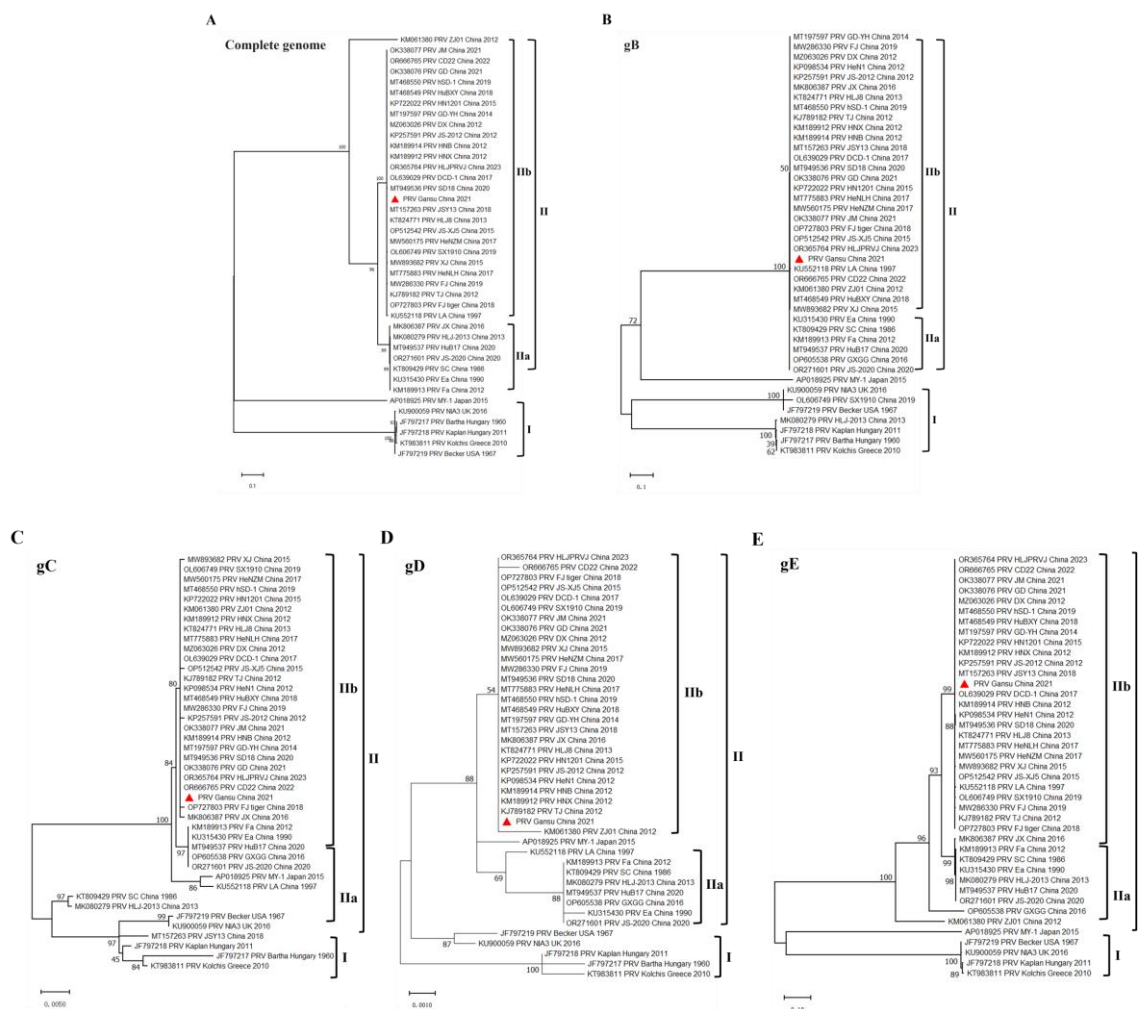


**Figure 5.** Phylogenetic analysis of the PRV strains. (A) Phylogenetic tree based on complete genomic nucleotide sequences. (B-E) Phylogenetic tree based on the nucleotide sequences of gB, gC, gD, and gE genes. Phylogenetic trees were constructed by using MEGA-X software with the ML method and bootstrapping with 1,000 replicates was performed to determine the percentage reliability for each internal node.

### 3.6. Pathogenicity of the PRV GS-2021 Strain in Mice

To investigate the pathogenicity of the PRV GS-2021 strain, all mice were challenged with the PRV GS-2021 strain at the dose of  $10^4$ ,  $10^3$ , and  $10^2$  PFU by I.N. injection, the Bartha-K61 vaccine strain and DMEM as a control. The results showed that the PRV GS-2021 strain was higher lethal to all mice, and the inoculated mice developed typical PRV symptoms such as severe itching, convulsions, and acute death in 2-3 days with the death rate reaching 100% (8/8) for  $10^4$  PFU and  $10^3$  PFU, and 37.5% (3/8) for  $10^2$  PFU (Table 5). The LD<sub>50</sub> of GS-2021 was  $10^{2.125}$  PFU/0.01ul that lower than those of Bartha-

K61 vaccine strain,  $10^{5.75}$  PFU/0.01ul (Table 5) (Figure 6A). However, all mice infected with the Bartha-K61 vaccine strain at 104 PFU did not appear obvious clinical symptoms, and one (1/8, 12.5%) and five mice (5/8, 62.5%) died in the infection dose of  $10^5$  and  $10^6$  PFU, respectively, at 14th day post-inoculation (Table 5) (Figure 6A). Additionally, histopathologic examinations showed that the PRV GS-2021 strain caused multiple lesion sites in the live, spleen or lung, such as local necrosis, apoptosis, congestion, and lymphocytes infiltrating (Figure 5B). Moreover, higher viral loads and PRV antigens-specific fluorescence signals were detected in blood, lung, spleen, liver, and brain from mice infected with the PRV GS-2021-infected group than the Bartha-K61 vaccine strain-infected group at 3 days post-infection (Figure 6C, D). These results, therefore, suggested the isolated PRV GS-2021 had a higher pathogenicity in mice.

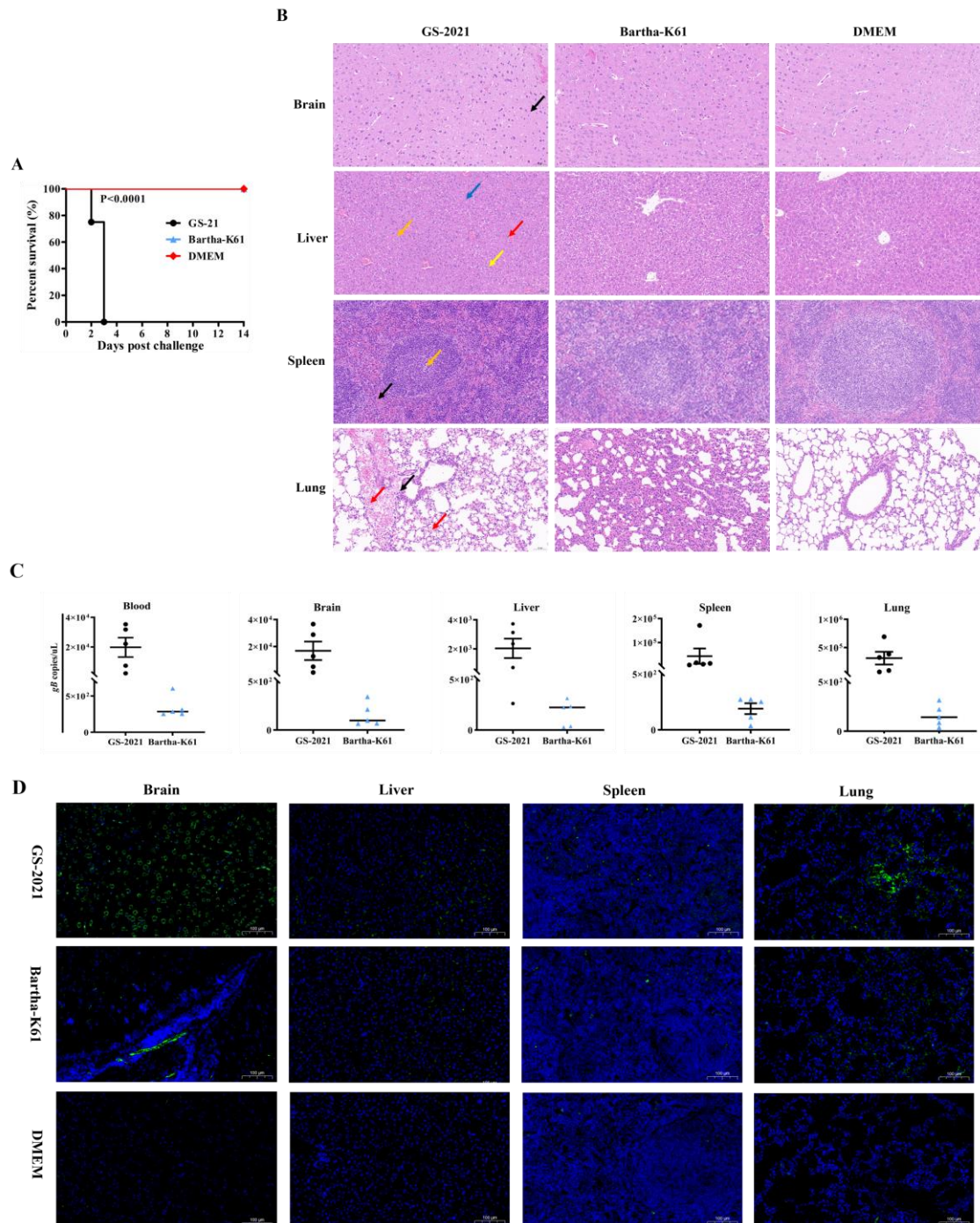


**Figure 6.** Pathogenicity of the PRV GS-2021 and Bartha-K61 strain in mice. (A) Kaplan-Meier survival curves of mice challenged with  $10^4$  PFU of GS-2021 and Bartha-K61 by intranasal routes ( $n=8$  in each group). (B) Histopathological changes in different tissues of mice infected with GS-2021. Paraffin sections of brain, liver,

spleen, and lung tissues from control,  $10^4$  PFU GS-2021, and  $10^4$  PFU Bartha-K61 groups were stained with hematoxylin and eosin (n=3 in each group). Infiltration of inflammatory cells (black arrows), hemorrhage (red arrows), local necrosis (orange arrows), vacuoles in the cytoplasm (yellow arrows), cell swelling and cytoplasm vacuolar (blue arrows). (C) PRV gB gene copies in blood, brain, liver, lung, and spleen samples of the mice intranasally challenged by GS-2021 and Bartha-K61, determined by gB-specific TaqMan real-time PCR. Each dot represents 1 mouse, and the data were collected and presented as mean  $\pm$  SEM from 5 mice in each group. (D) Identification of viral particles in brain, liver, lung, and spleen tissues by IFA analysis (n=3 in each group). Anti-PRV Polyclonal antibody was used as the primary antibody, and goat anti-rabbit IgG Alexa Fluor®488 (H+L) was used as the secondary antibody, and the nucleus was stained with DAPI.

**Table 5.** The LD50 values of the PRV strains in BALB/c mice.

Group	Mice number in each group	Dose (PFU)	Mortality	LD50
GS-2021	8	$10^4$	8/8	$10^{2.125}/0.01\text{ul}$
	8	$10^3$	8/8	
	8	$10^2$	3/8	
Bartha-K61	8	$10^6$	5/8	$10^{5.75}/0.01\text{ul}$
	8	$10^5$	1/8	
	8	$10^4$	0/8	
DMEM	8	/	0/8	/

#### 4. Discussion

PRV is a widely spread, highly pathogenic virus that infects multiple domestic and wild animals, and humans. The different PRV virus isolated strains the exhibited varied virulence and biological characteristics, although it still has only one strain type. Since late 2011, several emerging PRV variants have been identified in Bartha-K61-vaccinated pig farms, and then the variant strain rapidly spread to most regions of China and caused significant economic losses to the swine industry in China [3-6]. When compared to the foreign and Chinese classical PRV strains, the PRV variant strains shown higher virulence and pathogenicity and the Bartha-K61 vaccine strain fails to provide effective protection [3-5]. From 2012 to 2021, some reports showed that there was a high risk of the variant PRV strains substantial epidemic and the need for continuous monitoring [6-8]. Therefore, further understanding the biological and genetic characteristics of the prevalent PRV variant strains are important for preventing and controlling PR in China. However, it has always been debated whether the PRV variant strains currently persisting in Gansu Province of China, and its biological characteristics, genetic features, evolutionary relationship and pathogenicity are still unknown.

In the current study, a novel emerging field PRV variant strain called PRV/Gansu/China/2021 (PRV GS-2021) was successfully isolated and identified from the PRV-suspected clinical brain tissue sample of the dead piglets in a conventional Bartha-K61-vaccinated pig farm in Gansu Province of China, 2021, suggesting the PRV variant strain was already circulating in Gansu Province in China before 2021. Moreover, one-step growth curves revealed that the PRV isolated variant strain had similar growth characteristics with Bartha-K61 vaccine strains in vitro, but it grew to high titers in Vero cells. In particular, the PRV GS-2021 strain propagated slightly slower than the Bartha-K61 in PK-15 cells, suggesting the Bartha-K61 strain has a better ability to adapt to this cell line. However, the plaque diameter of the PRV GS-2021 strain was significantly bigger than that of Bartha-K61 in Vero cells. The results showed that the PRV GS-2021 strain had similar biological characteristics with previously isolated PRV variant strains. It is believed that several PRV infection cases in Gansu province of China in recent years were also caused by PRV variant strains, including the PRV GS-2021 variant strain.

At present, PRV strains prevalent worldwide are classified into clades I and II according to the phylogenetic and epidemiologic features [7]. Clades I mainly contain classical PRV strains from most regions of Europe and America, whereas clades II contain classical and variant PRV strains and

mainly prevalent in China [7]. The variant PRV strains are currently further classified into two sub-clades: Clades IIa, also known as classical PRV strains, which were more common before 2011 and Clades IIb, also known as novel PRV variants, which were first observed in late 2011 and since then have been dominant in China [7]. We found that the PRV GS-2021 strain belongs to clade II and was closely related to the variant strains in China (clade IIb) based on the gB, gC, gD, and gE genes sequences and the complete genome, respectively. As of now, it is believed that clade IIb remains the predominant epidemic clade affecting substantial economic losses in the pig industry in China, including Gansu province. Meanwhile, we found PRV GS-2021 strain showed high homology with clades II, including Chinese PRV variant strains and variant PRV strains, but it showed low homology with clades I, including Bartha-K61 vaccine strain, based on the nucleotide and amino acid sequence of gB, gC, gD, and gE genes and complete genome sequences of PRV. It is well known that the PRV gB, gC and gD proteins are the major immunogenetic antigens that can induce neutralizing antibody production [17-19]. Therefore, these results provided a possible explanation for why the Bartha-K61 vaccine strain provides only partial protection for PRV variants infection. Interestingly, two Aspartate (Asp) insertions are detected at sites 48 and 497 in the gE protein of the PRV Chinese variant strains, including the PRV GS-2021 strain, one Asp insertions are detected at sites 48 in the gE protein of the Chinese classical PRV strains, but Asp insertions are not discovered at sites 48 and 497 in the gE protein of the classical PRV strains in other countries, which are consistent with previously has been reported [4, 5, 20]. However, glutamate (Glu) is replaced by glycine (Gly) at position 91 only in the gE protein of the PRV GS-2021 strain that increased hydrophobicity of the gE protein. These results suggest that the insertion and/or substitution events in the gE protein of the PRV variants are not coincidental phenomenon, and that may be related to the host's immune pressure from the Bartha-K6 vaccine strain and may cause changes in pathogenicity and antigen characteristics of the PRV variant strains, including the PRV GS-2021 strain. Recently, several natural recombinant PRV variant strains were isolated and identified on Bartha-K61 vaccinated-pig farm and the natural recombination events maybe occurred in between different PRV genotypes or between wild-type strains and vaccine, although the recombination events were not detected in the PRV GS-2021 strain. Therefore, these results further explained that why the Bartha-K6 vaccine strain provides ineffective protection against the PRV variant strains, and it is necessary to continuously monitor the epidemiological trend and genetic evolution of PRV in China.

At the same time, it is interesting that the PRV GS-2021 strain clustered with two PRV variant strains named PRV/Xinjiang/China/2015 and PRV/Fujian/China/2018 from dog and tiger, respectively. Of note, more interspecies transmission events were observed with clade IIb PRV, including foxes, sheep, minks, raccoons and bovine, in recent years [1, 2, 6, 7, 21]. Importantly, a Chinese PRV variant strain called PRV/hSD-1/China/2019 was isolated from an acute human encephalitis case in 2019 and can effectively infect human cells and is genetically closest to those PRV variant strains currently circulating in pigs in China [15, 16]. Besides, since 2017, some reports shown that PRV might infect humans through detection of nucleic acids for PRV by PCR and metagenomic next-generation sequencing or PRV-gE/gB specific antibody by ELISA in China [11-14]. Moreover, it was previously reported that PRV gD has ability to bind human and swine-origin nectin-1 receptor with similar binding affinity to initiate virus entry into host cells [1, 2]. Therefore, these findings largely supported the close phylogenetic relationship and similar etiological characteristics of the PRV GS-2021 and hSD-1/2019 with other variant strains, suggesting the PRV variant strain is an emerging zoonotic pathogen that can infect humans in particular conditions and further implying the great risk of the PRV variant strains transmission from pigs to other animals, pigs to humans, humans to other animals or humans to humans. However, more information regarding the more PRV variant strains derived from human infection cases requires further investigation. For example, whether the different PRV strains have the different virulence and pathogenicity in humans and whether the current vaccines or antiviral drugs are safe and effective enough for humans to prevent novel PRV variants infections? And whether there is a correlation between PRV human infection cases and PRV infection level in pigs? Alternatively, whether the PRV GS-2021 strain can cross the species barrier and be transmitted to humans is unknown.

Furthermore, the pathogenicity of PRV GS-2021 strain was evaluated in mice in this study. All the infected mice died on the 3rd day, and typical PRV-caused symptoms were observed, when infected with  $10^4$  and  $10^3$  PFU of the PRV GS-2021. Even if infected with  $10^2$  PFU of the PRV GS-2021, three mice have only died on the 5th day after infection. In contrast, the all mice infected with  $10^4$  PFU Bartha-K61 vaccine strain exhibited normal behavior at 5th day post-infection, and did not cause the death of all mice at end of experiment at 14th day, although one and five mice died at 14th day post-inoculation in the infection dose of  $10^6$  and  $10^5$  PFU, respectively. In addition, the LD50 of the PRV GS-2021 strain is significantly lower than that of Bartha-K61 vaccine strain, which have also been reported in a previous study [22-24], indicating the PRV GS-2021 could a higher virulence variant strain. PRV DNA and antigens-specific fluorescence signals were further detected in different tissue samples from infected mice with 104 PFU of the PRV GS-2021 within 3 days post-infection. Moreover, the PRV GS-2021 strain infection in mice leads to encephalitis in brain including meningeal congestion, hemorrhage, edema and local necrosis, and multiple lesion sites such as, apoptosis, congestion, lymphocytes infiltrating in the live, spleen or lung, were observed by histopathological examination, suggested that the multiple organ damage with PRV infection may be the main cause of death in these mice. About the underlying mechanism involving multiple organ damage, we speculate that a break begins in the site of PRV infection, where the virus will replicate and then disseminate via the lymphatics and viraemia occurs when virus is released into the bloodstream, which then permits infection of the lung, spleen, brain and other organs and the virus replicates uncontrolled, the mice suffer multiple organ damage and most of them die. Notably, histopathologic examinations were normal in all tissues of the Bartha-K61 vaccine strain infected mice, which may be related to the infection route, dose and time, the virulence of the virus strain, and the age of animal model. Herein, we further demonstrated that the PRV GS-2021 strain is a higher virulence variant strain. However, the pathogenicity of the PRV GS-2021 strain and other different strains will be better evaluated in other animals, including pigs, bovine, sheep, and rhesus monkeys, in future experiments.

## 5. Conclusions

In summary, a novel emerging PRV variant strain, the PRV/Gansu/China/2021 (PRV GS-2021), was first isolated identified from a Bartha-K61-vaccinated pig farm in Gansu Province of China, 2021. The PRV GS-2021 strain is a higher virulence variant according to its etiological features, biological properties, phylogenetic relationships as well as pathogenicity in mice in our study and could have already circulated in Gansu Province before 2021. Our results will provide a theoretical reference for better understanding of the epidemiological and genetic evolutionary patterns of PRV and for novel vaccine design and control and prevention and eradication of PR in China.

**Author Contributions:** Conceptualization, Y.W. and Z.J.; methodology, X.H., H.Y., P.J., G.C. and Y.F.; software, X.H., P.J. and G.C.; validation, X.H. and H.Y.; formal analysis, X.H.; investigation, X.H., P.J., G.C. and Y.F.; data curation, X.H.; writing—original draft preparation, X.H.; writing—review and editing, X.H., P.J., Y.W. and Z.J.; visualization, X.H.; supervision, Y.W. and Z.J.; project administration, X.H. and H.Y.; funding acquisition, X.H. and H.Y. All authors have read and agreed to the published version of the manuscript.

**Funding:** This work was funded by the Natural Science Foundation of Gansu Province (No. 20JR10RA018), the 2022 Innovation Fund project of University Teachers (No. 2022B-357) and the Xinjiang Key Laboratory of Animal Infectious Diseases (No. 2023KLB003).

**Institutional Review Board Statement:** All animal experiments were handled in strict accordance with the Good Animal Practice Requirements of the Animal Ethics Procedures and Guidelines of the People's Republic of China, and the protocol was reviewed and approved by the Animal Ethics Committee of Lanzhou Veterinary Research Institute, Chinese Academy of Agricultural Science (Permission Number: LVRIAEC-2024-02-20).

**Informed Consent Statement:** Informed consent was obtained from all subjects involved in the study.

**Data Availability Statement:** All data presented in the present study can be found in online repositories.

**Conflicts of Interest:** The authors declare no conflicts of interest. The funders had no role in the design of the study; in the collection, analyses, or interpretation of data; in the writing of the manuscript; or in the decision to publish the results.

## References

1. Pomeranz, L.E.; Reynolds, A.E.; Hengartner, C.J. Molecular biology of pseudorabies virus: impact on neurovirology and veterinary medicine. *Microbiol. Mol. Biol. Rev.* **2005**, *69*, 462–500.
2. Szpara, M.L.; Tafuri, Y.R.; Parsons, L.; Shamim, S.R.; Verstrepen, K.J.; Legendre, M.; Enquist, L.W. A wide extent of inter-strain diversity in virulent and vaccine strains of alphaherpesviruses. *PLoS Pathog.* **2011**, *7*, e1002282.
3. Yu, X.L.; Zhou, Z.; Hu, D.M.; Zhang, Q.; Han, T.; Li, X.; Gu, X.X.; Yuan, L.; Zhang, S.; Wang, B.Y.; Qu, P.; Liu, J.H.; Zhao, X.Y.; Tian, K.G. Pathogenic pseudorabies virus, China, 2012. *Emerg. Infect. Dis.* **2014**, *20*, 102–104.
4. An, T.Q.; Peng, J.M.; Tian, Z.J.; Zhao, H.Y.; Li, N.; Liu, Y.M.; Chen, J.Z.; Leng, C.L.; Sun, Y.; Chang, D.; Tong, G.Z. Pseudorabies virus variant in Bartha-K61-vaccinated pigs, China, 2012. *Emerg. Infect. Dis.* **2013**, *19*, 1749–1755.
5. Luo, Y.Z.; Li, N.; Cong, X.; Wang, C.H.; Du, M.; Li, L.; Zhao, B.B.; Yuan, J.; Liu, D.D.; Li, S.; Li, Y.F.; Sun, Y.; Qiu, H.J. Pathogenicity and genomic characterization of a pseudorabies virus variant isolated from Bartha-K61-vaccinated swine population in China. *Vet. Microbiol.* **2014**, *174*, 107–115.
6. Tan, L.; Yao, J.; Yang, Y.D.; Luo, W.; Yuan, X.M.; Yang, L.C.; Wang, A.B. Current status and challenge of pseudorabies virus infection in China. *Virol. Sin.* **2021**, *36*, 588–607.
7. He, W.T.; Auclert, L.Z.; Zhai, X.F.; Wong, G.; Zhang, C.; Zhu, H.N.; Xing, G.; Wang, S.L.; He, W.; Li, K.M.; Wang, L.; Han, G.Z.; Veit, M.; Zhou, J.Y.; Suo, G. Interspecies transmission, genetic diversity, and evolutionary dynamics of pseudorabies virus. *J. Infect. Dis.* **2019**, *219*, 1705–1715.
8. Yang, Q.Y.; Sun, Z.; Tan, F.F.; Guo, L.H.; Wang, Y.Z.; Wang, J.; Wang, Z.Y.; Wang, L.L.; Li, X.D.; Xiao, Y.; Tian, K.G. Pathogenicity of a currently circulating Chinese variant pseudorabies virus in pigs. *World J. Virol.* **2016**, *5*, 23–30.
9. Sun, Y.; Luo, Y.; Wang, C.H.; Yuan, J.; Li, N.; Song, K.; Qiu, H.J. Control of swine pseudorabies in China: Opportunities and limitations. *Vet. Microbiol.* **2016**, *183*, 119–124.
10. Tan, L.; Zhou, Y.J.; Qiu, Y.X.; Lei, L.; Wang, C.; Zhu, P.; Duan, D.Y.; Lei, H.Y.; Yang, L.C.; Wang, N.D.; Yang, Y.; Yao, J.; Wang, W.; Wang, A.B. Pseudorabies in pig industry of China: Epidemiology in pigs and practitioner awareness. *Front. Vet. Sci.* **2022**, *9*, 973450.
11. Ai, J.W.; Weng, S.S.; Cheng, Q.; Cui, P.; Li, Y.J.; Wu, H.L.; Zhu, Y.M.; Xu, B.; Zhang, W.H. Human endophthalmitis caused by pseudorabies virus infection, China, 2017. *Emerg. Infect. Dis.* **2018**, *24*, 1087–1090.
12. Wong, G.; Lu, J.H.; Zhang, W.H.; Gao, G.F. Pseudorabies virus: a neglected zoonotic pathogen in humans? *Emerg. Microbes Infect.* **2019**, *8*, 150–154.
13. Chen, Y.M.; Gao, J.; Hua, R.Q.; Zhang, G.P. Pseudorabies virus as a zoonosis: scientific and public health implications. *Virus Genes* **2025**, *61*, 19–25.
14. Guo, Z.H.; Chen, X.X.; Zhang, G.P. Human PRV infection in China: an alarm to accelerate eradication of PRV in domestic pigs. *Virol. Sin.* **2021**, *36*, 823–828.
15. Liu, Q.Y.; Wang, X.J.; Xie, C.H.; Ding, S.F.; Yang, H.N.; Guo, S.B.; Li, J.X.; Qin, L.Z.; Ban, F.G.; Wang, D.F.; Wang, C.; Feng, L.X.; Ma, H.C.; Wu, B.; Zhang, L.P.; Dong, C.X.; Xing, L.; Zhang, J.W.; Chen, H.C.; Yan, R.Q.; Wang, X.R.; Li, W. A novel human acute encephalitis caused by pseudorabies virus variant strain. *Clin. Infect. Dis.* **2021**, *73*, e3690–e3700.
16. Peng, Z.; Liu, Q.Y.; Zhang, Y.B.; Wu, B.; Chen, H.C.; Wang, X.R. Cytopathic and genomic characteristics of a human-originated pseudorabies virus. *Viruses* **2023**, *15*, 170.
17. Bo, Z.Y.; Li, X.D. A Review of pseudorabies virus variants: genomics, vaccination, transmission, and zoonotic potential. *Viruses* **2022**, *14*, 1003.

18. Liu, Q.Y.; Kuang, Y.; Li, Y.F.; Guo, H.H.; Zhou, C.Y.; Guo, S.B.; Tan, C.; Wu, B.; Chen, H.C.; Wang, X.R. The epidemiology and variation in pseudorabies virus: a continuing challenge to pigs and humans. *Viruses* **2022**, *14*, 1463.
19. Tang, Y.D.; Liu, J.T.; Wang, T.Y.; Sun, M.X.; Tian, Z.J.; Cai, X.H. Comparison of pathogenicity-related genes in the current pseudorabies virus outbreak in China. *Sci. Rep.* **2017**, *7*, 7783.
20. Zhai, X.F.; Zhao, W.; Li, K.M.; Zhang, C.; Wang, C.C.; Su, S.; Zhou, J.Y.; Lei, J.; Xing, G.; Sun, H.F.; Shi, Z.Y.; Gu, J.Y. Genome characteristics and evolution of pseudorabies virus strains in eastern China from 2017 to 2019. *Virol. Sin.* **2019**, *34*, 601–609.
21. Cheng, Z.L.; Kong, Z.J.; Liu, P.; Fu, Z.D.; Zhang, J.D.; Liu, M.D.; Shang, L.Y. Natural infection of a variant pseudorabies virus leads to bovine death in China. *Transbound Emerg. Dis.* **2020**, *67*, 518–522.
22. Cheng, X.J.; Cheng, N.; Yang, C.; Li, X.L.; Sun, J.Y.; Sun, Y.F. Emergence and etiological characteristics of novel genotype pseudorabies virus variant with high pathogenicity in Tianjin, China. *Microb. Pathog.* **2024**, *197*, 107061.
23. Bo, Z.Y.; Miao, Y.Y.; Xi, R.; Gao, X.Y.; Miao, D.L.; Chen, H.; Jung, Y.Se.; Qian, Y.J.; Dai, J.J. Emergence of a novel pathogenic recombinant virus from Bartha vaccine and variant pseudorabies virus in China. *Transbound Emerg. Dis.* **2021**, *68*, 1454–1464.
24. Zhuang, L.L.; Gong, J.S.; Shen, J.Y.; Zhao, Y.; Yang, J.B.; Liu, Q.X.; Zhang, Y.; Shen, Q.P. Advances in molecular epidemiology and detection methods of pseudorabies virus. *Discov. Nano.* **2025**, *20*, 45.
- 25.
26. **Disclaimer/Publisher's Note:** The statements, opinions and data contained in all publications are solely those of the individual author(s) and contributor(s) and not of MDPI and/or the editor(s). MDPI and/or the editor(s) disclaim responsibility for any injury to people or property resulting from any ideas, methods, instructions or products referred to in the content.